

Phase diagram and excitations of a Shiba molecule

N. Y. Yao,¹ C. P. Moca,^{2,3} I. Weymann,⁴ J. D. Sau,⁵ M. D. Lukin,¹ E. A. Demler,¹ and G. Zaránd²

¹*Physics Department, Harvard University, Cambridge, Massachusetts 02138, USA*

²*BME-MTA Exotic Quantum Phase Group, Institute of Physics, Budapest University of Technology and Economics, H-1521 Budapest, Hungary*

³*Department of Physics, University of Oradea, 410087, Oradea, Romania*

⁴*Faculty of Physics, Adam Mickiewicz University, 61-614, Poznań, Poland*

⁵*Joint Quantum Institute and Condensed Matter Theory Center, Department of Physics, University of Maryland, College Park, Maryland 20742, USA*

(Received 12 May 2014; published 9 December 2014)

We analyze the phase diagram associated with a pair of magnetic impurities trapped in a superconducting host. The natural interplay between Kondo screening, superconductivity, and exchange interactions leads to a rich array of competing phases, whose transitions are characterized by discontinuous changes of the total spin. Our analysis is based on a combination of numerical renormalization group techniques as well as semiclassical analytics. In addition to the expected screened and unscreened phases, we observe a new molecular doublet phase where the impurity spins are only partially screened by a single extended quasiparticle. Direct signatures of the various Shiba molecule states can be observed via radio-frequency spectroscopy.

DOI: [10.1103/PhysRevB.90.241108](https://doi.org/10.1103/PhysRevB.90.241108)

PACS number(s): 75.30.Hx, 33.15.Kr, 75.30.Et

In an ordinary metal, the celebrated Kondo effect describes the scattering of conduction electrons due to magnetic impurities. Below the so-called Kondo temperature (T_K) [1], the magnetic moment of a single impurity becomes screened by the electrons [2], leading to its dissolution and, hence, the formation of a Fermi liquid state [3]. This simple picture can fail when one considers a finite density of impurities. In particular, conduction electrons mediate RKKY exchange interactions I between the impurities and, in the limit $I \gtrsim T_K$, such interactions can lead to the emergence of either magnetically ordered or spin glass states [4,5]. Much of our understanding of this phase transition owes to detailed studies of the two-impurity Kondo model [6,7].

Extending the two-impurity calculations to the case of a superconducting host represents an interesting and active challenge [8–17]. On the one hand, the interplay of superconductivity and magnetic moments can lead to the emergence of exotic phases and excitations. Recent results have suggested the possibility of emergent Majorana edge modes at the ends of a magnetic impurity chain situated on the surface of an s -wave superconductor; in this system, topological superconductivity arises from the formation of a spin helix as a result of the underlying RKKY interaction [18–20]. On the other hand, the presence of magnetic impurities breaks time-reversal symmetry and gradually leads to the destruction of superconductivity. This breakdown occurs through the appearance of proliferating midgap states (so-called Shiba states), as first observed by Yu, Shiba, and Rusinov [21–23]. In particular, within a simple classical calculation, they demonstrated that a magnetic impurity can bind an antialigned quasiparticle, yielding a subgap bound state of energy $\epsilon = \Delta - E_b$, where Δ represents the superconducting gap and E_b the binding energy [24–26]. As the binding energy E_b increases (e.g., as a function of increasing exchange coupling), the bound state energy eventually crosses zero, signifying a parity-changing phase transition.

With certain modifications, this classical picture remains qualitatively valid even for quantum-mechanical spins

[15,27–31]. Taking into account quantum fluctuations, the aforementioned parity-changing transition occurs at a critical point, $(\Delta/T_K)_c$, when the superconducting gap becomes comparable to the Kondo temperature [2]. For an $S = 1/2$ impurity, the spin is essentially free for $\Delta/T_K > (\Delta/T_K)_c$ and the associated midgap Shiba state remains unoccupied. In this “free spin” regime, the ground state has spin $S_G = 1/2$. In the opposite limit, when $\Delta/T_K < (\Delta/T_K)_c$, the impurity spin becomes screened by a bound quasiparticle; more specifically, the midgap Shiba state becomes occupied and this quasiparticle spin forms a singlet with the impurity spin, leading to an $S_G = 0$ ground state. This phase transition has recently been observed in mesoscopic circuits, where the strength of the exchange interaction can be tuned by means of a pinch-off gate electrode [32,33].

In this Rapid Communication, we use a combination of numerical renormalization group methods and semiclassical analytics to study quantum phases of two magnetic impurities in a superconductor. We first identify all possible phases, and construct the superconducting analog of Doniach’s fundamental phase diagram [34]. To this end, we demonstrate the existence of bound “molecular” quasiparticle states, delocalized between the magnetic impurities, and also elucidate a

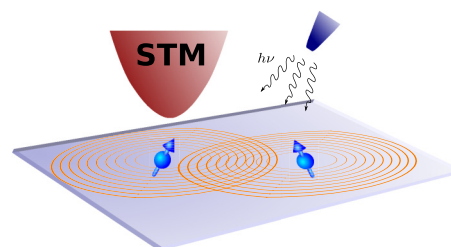


FIG. 1. (Color online) Two magnetic impurities placed on a superconducting surface. Radio-frequency fields can be used to produce transitions between various molecular states and manipulate them.

novel singlet state with two bound quasiparticles. We explore and characterize the experimental signatures of the phase transitions between all observed phases, and demonstrate the presence of multiple Shiba states and universal weight jumps in the STM spectrum.

We consider an s -wave superconductor with Hamiltonian

$$H_{\text{BCS}} = \int \frac{d\mathbf{k}}{(2\pi)^3} \left[\sum_{\sigma} \xi_{\mathbf{k}} c_{\mathbf{k}\sigma}^{\dagger} c_{\mathbf{k}\sigma} + (\Delta c_{\mathbf{k}\uparrow}^{\dagger} c_{-\mathbf{k}\downarrow}^{\dagger} + \text{H.c.}) \right]$$

coupled, via exchange, to two identical spin-1/2 magnetic impurities of spin \mathbf{S}_1 and \mathbf{S}_2 ,

$$H_{\text{int}} = \frac{J}{2} \mathbf{S}_1 \psi_1^{\dagger} \boldsymbol{\sigma} \psi_1 + \frac{J}{2} \mathbf{S}_2 \psi_2^{\dagger} \boldsymbol{\sigma} \psi_2. \quad (1)$$



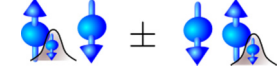

Here, ψ_1 and ψ_2 are the field operators at the impurity positions. We note that this Hamiltonian captures the essential physics of two experimental systems: (1) magnetic impurities placed on a superconducting surface (see Fig. 1) [24,26,35] and (2) double dot devices attached to superconductors (e.g., as recently used for Cooper pair splitting) [36,37]. To study the ground state and excitation spectrum of $H_T = H_{\text{BCS}} + H_{\text{int}}$, we map the problem to a double superconducting chain, and analyze it via Wilson's numerical renormalization group (NRG) method [6]. Details of our NRG calculation are provided in [38].

We observe that H_T conserves both parity P and total spin S . In a superconductor, the pairing terms imply that charge is typically only conserved modulo 2. However, for $\Delta = 0$ and in the presence of particle-hole symmetry, the Wilson chain possesses a hidden $\text{SU}_c(2)$ charge symmetry [6] analogous to that of the Hubbard model [39]. For a half-filled cubic lattice, this charge symmetry is generated by the operators, $Q_x = (Q^+ + Q^-)/2$, $Q_y = (Q^+ - Q^-)/2i$, $Q^z = \frac{1}{2} \sum_{\sigma} \int \frac{d\mathbf{k}}{(2\pi)^3} (c_{\mathbf{k}\sigma}^{\dagger} c_{\mathbf{k}\sigma} - \frac{1}{2})$, where $Q^+ = \int \frac{d\mathbf{k}}{(2\pi)^3} c_{\mathbf{k}\uparrow}^{\dagger} c_{\pi-\mathbf{k}\downarrow}^{\dagger}$ and $Q^- = (Q^+)^{\dagger}$ [40]. Although this symmetry is strictly broken for $\Delta \neq 0$, a hidden $U_c(1)$ symmetry remains, leading to a conserved pseudocharge \tilde{Q} [38,41]. Physically, this pseudocharge can be viewed as the generator of rotations along the superconducting order parameter. For the remainder of the text, we will utilize these three quantum numbers (P , S , and \tilde{Q}) to classify the eigenstates of the Hamiltonian.

Our NRG calculations reveal the existence of five competing subgap Shiba-molecule states, as depicted in Table I. For large values of Δ , both of the impurity spins are essentially free.

They can form a singlet state (S_0) with spin $S = 0$, parity $P = -$, and pseudocharge $\tilde{Q} = 0$, or a triplet state (T_0) with $S = 1$, $P = +$, and $\tilde{Q} = 0$. Similar to the single impurity case, one can also create a single (antiferromagnetically) bound quasiparticle. However, in the Shiba molecule case, this quasiparticle is delocalized between the two impurities and can form either a bonding (D_+) or antibonding state (D_-) of spin $S = 1/2$, parity $P = \pm$, and pseudocharge $\tilde{Q} = 1$. Finally, it is also possible to induce the binding of two quasiparticles, one to each of the impurities. In this case, one finds a singlet state (S_2) with pseudocharge $\tilde{Q} = 2$. The parity of this state is, rather counterintuitively, $P = -$, owing to the fermionic nature of the bound quasiparticles.

TABLE I. (Color online) Shiba molecular bound states and their quantum numbers. Small spins represent quasiparticles bound to the (large) impurity spins.

State	(S, \tilde{Q}, P)
	(0,0,-)
	(1,0,+)
	($\frac{1}{2}$,1, \pm)
	(0,2,-)

The competition between these five states leads to a rich Shiba molecule phase diagram. A heuristic understanding of this diagram can be gained by comparing the relative strengths of superconductivity, exchange, and Kondo screening. In analogy to the single-impurity case, the ratio Δ/T_K characterizes the competition between superconductivity and Kondo screening. For $\Delta/T_K \gg 1$, Kondo screening is heavily suppressed and the magnetic moments remain unscreened. The two impurities do, however, couple to each other via the Fermi sea of conduction electrons. For processes involving quasiparticle excitations close to the Fermi energy, this coupling is characterized by the overlap \mathcal{S} of the two waves created at the impurity locations. For a three-dimensional free electron system, $\mathcal{S} = \frac{\sin(k_F R)}{k_F R}$, where $R = |\mathbf{R}_1 - \mathbf{R}_2|$ is the separation between the impurities and k_F the Fermi momentum. This overlap \mathcal{S} is also responsible for the hybridization of the Shiba states at sites 1 and 2, and thus for the splitting between the bonding and antibonding states (D_{\pm}).

The impurity spins also interact via RKKY exchange I , which depends on high-energy electron-hole excitations; thus, the coupling I ought be considered as an independent parameter, determined by the precise band shape and the energy dependence of the exchange coupling J . The competition between RKKY and Kondo screening is characterized by the ratio I/T_K [42].

Phase diagram. The phase diagram obtained via NRG is shown in Fig. 2. We identify four distinct regions, each corresponding to one of the states in Table I.

(1) For large values of Δ/T_K , the impurities are free and the ground state is a *molecular triplet* (T_0) for $I < 0$ and a *molecular singlet* (S_0) for $I > 0$. As expected, this molecular singlet phase is also observed for $I \gg T_K, \Delta$ and extends down to the $\Delta = 0$ axis.

(2) In the *Kondo singlet* region (S_2), $|I|, \Delta \ll T_K$, one recovers strong Kondo correlations, wherein the two impurity spins are basically individually screened by quasiparticles. For perfect electron-hole symmetry, this region is separated from (1) by a first-order phase transition (blue dashed line in Fig. 2), corresponding to both a pseudocharge jump from $\tilde{Q} = 0$ to $\tilde{Q} = 2$ as well as a $S_0 \rightarrow S_2$ singlet-singlet level crossing. When electron-hole symmetry is broken, the transition becomes a smooth crossover.

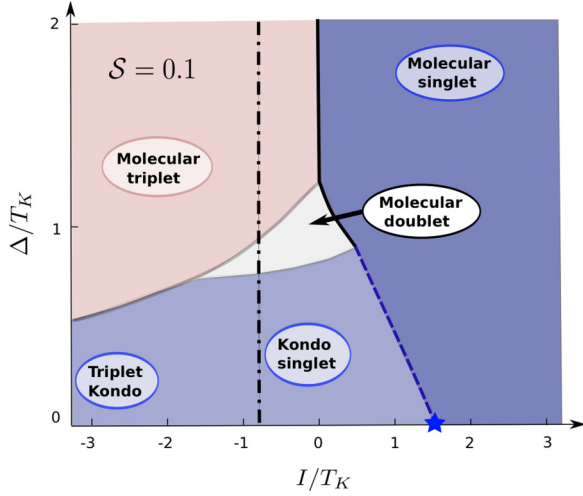


FIG. 2. (Color online) NRG-determined phase diagram for $S = 0.1$ as function of I/T_K and Δ/T_K . The background colors indicate regions with $S = 1$ (light maroon), $S = 1/2$ (white), and $S = 0$ (blue) ground states. The blue dashed line separates the regions with S_2 (light blue) and S_0 (dark blue) ground states. All phase transitions are first order, except the blue dashed line, which becomes a smooth crossover in the absence of electron-hole symmetry. The observed first-order transitions are in contrast to the quantum phase transitions observed in the two-channel and two-impurity Kondo models (whose quantum critical point is indicated by the blue star), where local correlation functions exhibit critical behavior with a nontrivial exponent.

(3) Along the $\Delta = 0$ line, the known phase diagram of the two impurity (normal metal) Kondo model is recovered [5]. Here, a quantum critical point (blue star) separates the molecular singlet from the Kondo singlet region. For any finite Δ , the spectrum is gapped, and this critical point turns into the aforementioned first-order transition line.

The nature of the Kondo singlet phase at $\Delta = 0$ gradually changes as one moves toward large, negative exchange interactions. In particular, for $-I \gg T_K$, the two impurity spins are first bound into a molecular triplet, which is then screened in the even and odd channels at (typically) two different Kondo temperatures. This picture survives for small but finite Δ , although strictly speaking, there is no true Kondo effect for any finite gap; nevertheless, one can still screen the impurity spins for $\Delta \ll T_K$ and a Kondo anomaly is generally observed in the tunneling spectra at intermediate energies, $\Delta \ll \omega \ll T_K$.

(4) Finally, and most strikingly, for $S \neq 0$, a new $S = 1/2$ phase emerges for $\Delta \sim T_K$ and $I \approx 0$. We term this phase the *molecular doublet* (D_+). It can be understood as follows. For $\Delta \gg T_K$, each of the two spins can bind a single excited quasiparticle. For $S = 0$, the energies of these bound states are identical; however, for $S \neq 0$, these states can hybridize to form molecular bonding and antibonding states D_{\pm} . As one decreases the ratio Δ/T_K , the energy of the D_{\pm} states moves towards zero until D_+ first crosses (zero) and becomes the ground state. This transition is accompanied by a charge-parity flip and a spin transition from $S = 1 \rightarrow 1/2$. Further decreasing Δ/T_K lowers the energy of the two-bound-quasiparticle state until a second charge parity transition to the S_2 singlet occurs. These level crossings and the evolution of

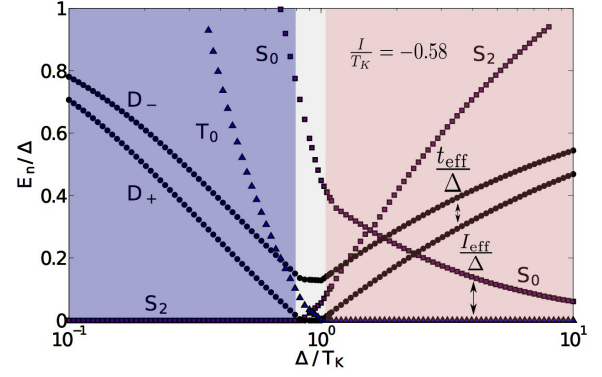


FIG. 3. (Color online) Evolution of the bound states as function of Δ/T_K for RKKY couplings $I/T_K = -0.58$ and an overlap parameter $S = 0.1$ and corresponds to the black dashed line in Fig. 2. One observes a phase transition from the *individual singlet* state (S_2) into the *molecular doublet* phase (D_+) and then another transition to the *molecular triplet* phase (T_0). The effective RKKY interaction can be extracted as the splitting between the S_0 and T_0 states: $I_{\text{eff}} = E_{S_0} - E_{T_0}$. We can also estimate the effective hopping t_{eff} as the separation between the two molecular doublet states, D_{\pm} .

the excitation spectrum along the vertical dash-dotted line in Fig. 2 is shown in Fig. 3. Interestingly, an analogous doublet phase is found when considering the full Anderson model [43].

The existence of this novel molecular doublet phase can also be probed and confirmed in a semiclassical calculation where one extends the original Yu-Shiba-Rusinov calculation to the case of two classical magnetic impurities. Each magnetic impurity binds a Shiba state with wave function $\phi_{\text{sh}}(\mathbf{r}) \sim \frac{1}{r} e^{-r/\zeta} |\sin(2\delta)|$ and energy $E_{\text{sh}} = \Delta \frac{1-\beta^2}{1+\beta^2}$, where ζ is the coherence length, $\beta \equiv \tan(\delta) = JSN_0\pi/2$, and N_0 is the density of states at the Fermi energy. Utilizing a two-impurity Green's function calculation [44,45], we compute the energies of the hybridized Shiba bound states as poles of the T matrix [38]. Picking two values of $k_F R$ (corresponding to ferromagnetic and antiferromagnetic exchange) we plot the bound-state energies as a function of β (Fig. 4). In each case, hybridization causes a single bound state to first cross $E_{\text{sh}} = 0$ leading to the formation of the molecular doublet phase. The second bound-state crossing then yields the transition to either the triplet Kondo phase ($I < 0$) or the Kondo singlet phase ($I > 0$).

Tunneling rf spectroscopy. The most direct observation of the various molecular Shiba states can be achieved by combining rf spectroscopy with transport measurements. To this end, we determine the tunneling spectrum of the Shiba molecule by computing the spectral density of the so-called composite fermion, $F_1 \equiv \mathbf{S}_1 \cdot \boldsymbol{\sigma} \psi_1$. In the molecular triplet phase (T_0), both D_+ and D_- are visible in the tunneling spectrum and, correspondingly, a double midgap STM resonance is predicted (see Fig. 5). The dominant obstacle to observing such a resonance arises from thermal broadening; indeed, the first such measurements of Mn and Gd impurities [46] on a single-crystal lead superconductor at ~ 4 K were unable to resolve individual Shiba resonances [24]. Recently, however, multiple Shiba states were detected for Mn impurities on a superconducting Pb surface [25,47]. Operating at even lower

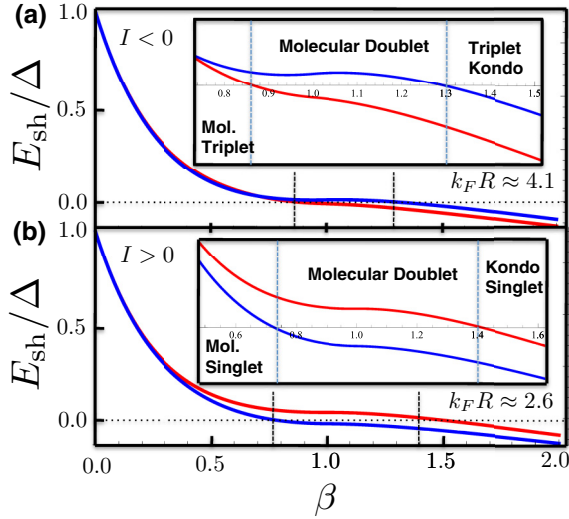


FIG. 4. (Color online) Semiclassical molecular doublet phase transitions. (a) For $k_F R \approx 4.1$, the RKKY exchange is negative and the bound state energies are shown as one increases $\beta = JN S \pi / 2$. At $\beta \approx 0.86$, the first bound state crosses zero and a charge-parity transition from the molecular triplet phase to the doublet phase occurs. At $\beta \approx 1.3$, the second bound state crossing leads to the triplet Kondo phase. (b) Analogous semiclassical results for $k_F R \approx 2.6$ where the exchange is positive.

temperatures (~ 500 mK) the linewidth is reduced considerably to ≈ 0.14 meV, significantly smaller than the superconducting gap, $\Delta_{\text{pb}} = 1.55$ meV. Such estimates are consistent with recent results that utilize a superconducting Niobium tip to explicitly resolve multiple Shiba scattering channels [26,48]. Even lower temperatures, in the range of $T \sim 20$ mK, can be attained in mesoscopic circuits, where multiple Shiba states have also been recently resolved [49].

Applying an additional rf field with a frequency matched to the $T_0 \rightarrow S_0$ transition ($\Delta E = h\nu$) allows one to populate the S_0 state [50]. In this case, the $S_0 \rightarrow D_{\pm}$ transitions also become active and visible (Fig. 5), while the tunneling gap shifts from $\Delta \rightarrow \Delta - \Delta E$. In this way, one can detect the excited state S_0 and its energy by investigating the rf-radiation-induced transport signal.

The transitions between the various phases and the corresponding STM spectra should also be observable in double-dot spin-splitter devices. In particular, the tunneling dI/dV spectra can be accessed by observing the transport with normal electrodes attached. Similar to the case of a simple magnetic impurity, by approaching the phase boundaries

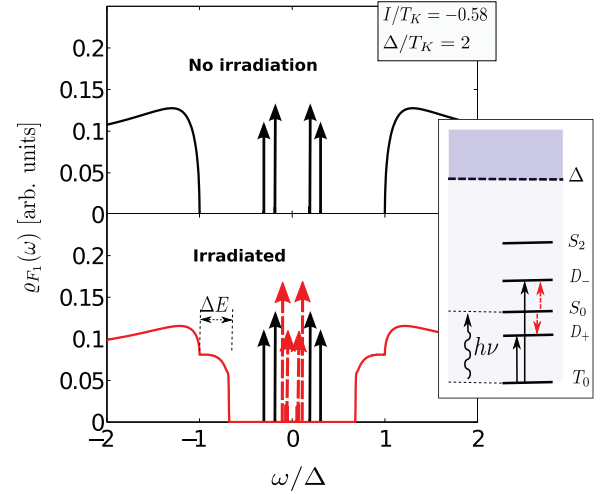


FIG. 5. (Color online) STM spectrum of one atom of the Shiba molecule in the molecular triplet (T_0) phase. The D_+ and the D_- states can both be observed as subgap Shiba transition lines (see top). Upon irradiation with a frequency matching the $T_0 \rightarrow S_0$ transition $h\nu = \Delta E$ (right panel), two additional subgap lines appear, and the gap shifts to lower values (bottom).

between (D_+, S_2) or (D_+, T_0), a single midgap excitation should get “soft” and cross zero. Interestingly, the strength of the corresponding tunneling resonance displays a *universal jump* at these transitions, $2 \rightarrow 1$ and $3 \rightarrow 2$, respectively; this robust jump owes to a change in ground-state degeneracy [32].

As a possible application, one can consider using the singlet states S_2 and S_0 as a quantum bit. These states are protected by the superconducting gap and, being singlets, they are insensitive to magnetic noise (including the hyperfine field of nearby nuclear moments) [51]. To have a direct transition between these states, both parity and particle-hole symmetry must be broken sufficiently strongly; this can be achieved by placing a single potential scatterer near one of the magnetic impurities, as may be possible in STM-type experiments [24,26,48].

We thank Leonid Glazman for insightful comments and lively discussions. This work is supported in part by the Hungarian research fund OTKA under Grant Nos. K105149, CNK80991, the UEFISCDI grant DYMESYS (PN-II-ID-JRP-2011-1), the “Iuventus Plus” project No. IP2011 059471, the EU Grant No. CIG-303 689, the DOE (FG02-97ER25308), the Harvard-MIT CUA, the ARO-MURI on Atomtronics, and the ARO MURI Quism program. Computing time at Poznań Superconducting and Networking Center is acknowledged.

- [1] Hereafter, T_K denotes the Kondo temperature in the normal phase. For a precise definition, see [38].
- [2] A. Hewson, *The Kondo Problem to Heavy Fermions* (Cambridge University Press, New York, NY, 1993).
- [3] P. Nozieres, *J. Low Temp. Phys.* **17**, 31 (1974).

- [4] H. Tsunetsugu, M. Sigrist, and K. Ueda, *Rev. Mod. Phys.* **69**, 809 (1997).
- [5] S. Doniach, *Physica B+C* **91**, 231 (1977).
- [6] B. A. Jones and C. M. Varma, *Phys. Rev. Lett.* **58**, 843 (1987).
- [7] I. Affleck and A. W. W. Ludwig, *Phys. Rev. Lett.* **68**, 1046 (1992).

- [8] D. Poilblanc, D. J. Scalapino, and W. Hanke, *Phys. Rev. Lett.* **72**, 884 (1994).
- [9] A. V. Balatsky, M. I. Salkola, and A. Rosengren, *Phys. Rev. B* **51**, 15547 (1995).
- [10] M. E. Flatté and J. M. Byers, *Phys. Rev. Lett.* **78**, 3761 (1997).
- [11] M. E. Flatté and J. M. Byers, *Phys. Rev. B* **56**, 11213 (1997).
- [12] M. I. Salkola, A. V. Balatsky, and J. R. Schrieffer, *Phys. Rev. B* **55**, 12648 (1997).
- [13] M. E. Flatté and D. E. Reynolds, *Phys. Rev. B* **61**, 14810 (2000).
- [14] S. H. Pan, E. W. Hudson, K. M. Lang, H. Eisaki, S. Uchida, and J. C. Davis, *Nature (London)* **403**, 746 (2000).
- [15] A. V. Balatsky, I. Vekhter, and J.-X. Zhu, *Rev. Mod. Phys.* **78**, 373 (2006).
- [16] C. P. Moca, E. Demler, B. Jankó, and G. Zaránd, *Phys. Rev. B* **77**, 174516 (2008).
- [17] Y. V. Fominov, M. Houzet, and L. I. Glazman, *Phys. Rev. B* **84**, 224517 (2011).
- [18] M. Ruderman and C. Kittel, *Phys. Rev.* **96**, 99 (1954).
- [19] T. Kasuya, *Prog. Theor. Phys.* **16**, 45 (1956).
- [20] K. Yosida, *Phys. Rev.* **106**, 893 (1957).
- [21] Y. Luh, *Acta Phys. Sin.* **21**, 75 (1965).
- [22] H. Shiba, *Prog. Theor. Phys.* **40**, 435 (1968).
- [23] A. I. Rusinov, *Zh. Eksp. Teor. Fiz.* **56**, 2047 (1969) [*Sov. Phys. JETP* **29**, 1101 (1969)].
- [24] A. Yazdani, B. A. Jones, C. P. Lutz, M. F. Crommie, and D. M. Eigler, *Science* **275**, 1767 (1997).
- [25] K. J. Franke, G. Schulze, and J. I. Pascual, *Science* **332**, 940 (2011).
- [26] S.-H. Ji, T. Zhang, Y.-S. Fu, X. Chen, X.-C. Ma, J. Li, W.-H. Duan, J.-F. Jia, and Q.-K. Xue, *Phys. Rev. Lett.* **100**, 226801 (2008).
- [27] T. Hecht, A. Weichselbaum, J. von Delft, and R. Bulla, *J. Phys.: Condens. Matter* **20**, 275213 (2008).
- [28] T. Meng, S. Florens, and P. Simon, *Phys. Rev. B* **79**, 224521 (2009).
- [29] P. Stadler, C. Holmqvist, and W. Belzig, *Phys. Rev. B* **88**, 104512 (2013).
- [30] J. Bauer, A. Oguri, and A. C. Hewson, *J. Phys.: Condens. Matter* **19**, 486211 (2007).
- [31] R. Žitko, O. Bodensiek, and T. Pruschke, *Phys. Rev. B* **83**, 054512 (2011).
- [32] R. S. Deacon, Y. Tanaka, A. Oiwa, R. Sakano, K. Yoshida, K. Shibata, K. Hirakawa, and S. Tarucha, *Phys. Rev. Lett.* **104**, 076805 (2010).
- [33] E. J. Lee, X. Jiang, M. Houzet, R. Aguado, C. M. Lieber, and S. De Franceschi, *Nat. Nano* **9**, 79 (2014).
- [34] Some related results in the limit of $\Delta \ll T_K$ and vanishing overlap \mathcal{S} have been obtained in Ref. [31].
- [35] M. Iavarone, G. Karapetrov, J. Fedor, D. Rosenmann, T. Nishizaki, and N. Kobayashi, *J. Phys.: Condens. Matter* **22**, 015501 (2010).
- [36] L. Hofstetter, S. Csonka, J. Nygard, and C. Schonenberger, *Nature (London)* **461**, 960 (2009).
- [37] L. G. Herrmann, F. Portier, P. Roche, A. L. Yeyati, T. Kontos, and C. Strunk, *Phys. Rev. Lett.* **104**, 026801 (2010).
- [38] See Supplemental Material at <http://link.aps.org/supplemental/10.1103/PhysRevB.90.241108> for methods and theoretical derivations.
- [39] F. H. L. Essler, H. Frahm, F. Ghmman, A. Klmpfer, and V. E. Korepin, *The One-Dimensional Hubbard Model* (Cambridge University Press, Cambridge, UK, 2005).
- [40] Here π denotes the corner of the Brillouin zone.
- [41] T. Yoshioka and Y. Ohashi, *J. Phys. Soc. Jpn.* **69**, 1812 (2000).
- [42] In the NRG scheme, a direct interaction between the impurities must also be introduced (see Refs. [38] and [6]).
- [43] R. Žitko, M. Lee, R. López, R. Aguado, and M.-S. Choi, *Phys. Rev. Lett.* **105**, 116803 (2010).
- [44] N. Y. Yao, L. I. Glazman, E. A. Demler, M. D. Lukin, and J. D. Sau, *Phys. Rev. Lett.* **113**, 087202 (2014).
- [45] F. Pientka, L. I. Glazman, and F. von Oppen, *Phys. Rev. B* **88**, 155420 (2013).
- [46] Both Mn and Gd are high spin magnetic impurities. Adding in such effects (e.g., of single-ion anisotropy) is an interesting direction [31].
- [47] J. Bauer, J. I. Pascual, and K. J. Franke, *Phys. Rev. B* **87**, 075125 (2013).
- [48] S.-H. Ji, T. Zhang, Y.-S. Fu, X. Chen, J.-F. Jia, Q.-K. Xue, and X.-C. Ma, *Appl. Phys. Lett.* **96**, 073113 (2010).
- [49] A. Kumar, M. Gaim, D. Steining, A. Levy Yeyati, A. Matrin-Rodero, A. K. Hüttl, and C. Strunk, *Phys. Rev. B* **89**, 075428 (2014).
- [50] Parity must be broken to induce a $S_0 \rightarrow T_0$ transition, e.g., by an inhomogeneous magnetic field.
- [51] N. Y. Yao *et al.* (unpublished).